HHS Public Access

Author manuscript

Am J Geriatr Psychiatry. Author manuscript; available in PMC 2020 February 28.

Published in final edited form as:

Am J Geriatr Psychiatry. 2019 December ; 27(12): 1360–1371. doi:10.1016/j.jagp.2019.07.008.

Relationships Between Executive Control Circuit Activity, Amyloid Burden, and Education in Cognitively Healthy Older Adults

Helmet T. Karim, Ph.D.[1],
Department of Psychiatry, University of Pittsburgh, Pittsburgh, PA

Dana L. Tudorascu, Ph.D.[1],
Department of Psychiatry, University of Pittsburgh, Pittsburgh, PA

Department of Internal Medicine, University of Pittsburgh, Pittsburgh, PA

Department of Biostatistics, University of Pittsburgh, Pittsburgh, PA

Ann Cohen, Ph.D.,
Department of Psychiatry, University of Pittsburgh, Pittsburgh, PA

Julie C. Price, Ph.D.,
Department of Radiology, Massachusetts General Hospital, Boston, MA

Brian Lopresti, M.Sc.,
Department of Radiology, University of Pittsburgh, Pittsburgh, PA

Chester Mathis, Ph.D.,
Department of Radiology, University of Pittsburgh, Pittsburgh, PA

William Klunk, M.D., Ph.D.,
Department of Radiology, University of Pittsburgh, Pittsburgh, PA

Department of Neurology, University of Pittsburgh, Pittsburgh, PA

Beth E. Snitz, Ph.D.,
Department of Neurology, University of Pittsburgh, Pittsburgh, PA

Howard J. Aizenstein, M.D., Ph.D.
Department of Psychiatry, University of Pittsburgh, Pittsburgh, PA

Department of Bioengineering, University of Pittsburgh, Pittsburgh, PA

Abstract

Introduction—In cognitively healthy older adults, amyloid-beta (Aβ) burden is associated with greater activity on task-based functional magnetic resonance imaging. Higher levels of functional activation are associated with other factors along with amyloid and the authors investigated these relationships as well as how they relate to Aβ in cognitively healthy older adults.

Send correspondence and reprint requests to Howard Aizenstein, M.D., Ph.D., Department of Psychiatry, University of Pittsburgh, 3811 O'Hara St., Pittsburgh, PA 15213.aizen@pitt.edu.

[1]Equal contribution to this manuscript.

Methods—The authors recruited cognitive healthy older adults (N = 50) from the Pittsburgh community that underwent extensive cognitive batteries, activation during a working memory (digit symbol substitution task, DSST), positron emission tomography scan for Pittsburgh Compound B (PiB, measuring amyloid), and other demographic measures. The authors tested the association between DSST activation and global PiB, neurocognitive batteries, and education.

Results—The authors found that the DSST robustly activated expected structures involved in working memory. The authors found that greater global Ab deposition was associated with greater DSST activation in the right calcarine, precuneus, middle temporal as well as the left insula and inferior frontal gyrus. The authors also found that greater education was associated with lower DSST activation - however this was not significant after adjusting for Ab.

Discussion—Greater amyloid was associated with greater activation, which may represent compensatory activation. Greater education was associated with lower activation, which may represent more efficient activation (i.e., less activation for the same task). After adjusting for amyloid, education was not significantly associated with activation suggesting that during the preclinical stage amyloid is the primary determinant of activation. Further, activation was not associated with cognitive function. Compensatory activation in the preclinical stage may help maintain cognitive function.

Keywords

Amyloid; PiB; DSST; fMRI; cognitive reserve

INTRODUCTION

Amyloid-beta (Aβ) protein is a key marker in the pathology of Alzheimer disease (AD) and is associated with atrophy, decreases in glucose metabolism, worsening cognitive function, and changes in brain activation and connectivity.[1–4] Previous studies have shown an accumulation of Aβ in preclinical AD and may reflect early manifestation of AD pathology.[5,6] A three-stage model for AD has been described: initial Aβ deposition, followed by neurodegeneration (including synaptic degeneration, neural atrophy, hypometabolism, and changes in connectivity), and finally progressive cognitive dysfunction.[7] This has resulted in interest in preclinical AD and attempts to detect early biomarkers of AD progression as well as disease prevention.[8]

In cross-sectional studies in older cognitively normal (CN) participants, cognitive functioning is marginally associated with Aβ. A meta-analysis found a small association with episodic memory.[8] In contrast, most longitudinal studies report associations between Aβ deposition and cognitive decline,[9–12] which is stronger in the presence of biomarkers of neurodegeneration.[13,14]

Aβ deposition is strongly associated with brain metabolism as well as functional activation.[15–21] In task-based functional magnetic resonance imaging (fMRI) studies, higher Aβ burden in CN older adults is associated with increased activation during memory encoding, along with other tasks like language processing, fluency, and face processing.[19,22,23] Most notably, these studies suggest increased activation within the hippocampus during memory

encoding,[23] possibly reflecting compensatory hippocampal activation. Greater activation (e.g., compensation) may explain the absence of a strong association between cognitive functioning and Aβ in CN but Aβ-positive older adults.[18]

Individuals with greater education have been shown to have lower activation, which may be due to more efficient neural activation patterns.[24] Education is one such proxy for cognitive reserve - or the capacity to maintain healthy cognitive function in the presence of pathology. Cognitive reserve has been traditionally measured with level of education, premorbid IQ, and occupational attainment as these have been correlated with lower levels of activation in healthy individuals and a lower risk for developing pathology (e.g., AD).[25] Cognitive reserve may explain the variability in individual susceptibility to pathology − where some individuals with relatively high levels of amyloid do not present with AD symptoms and some individuals with relatively mild levels of amyloid have memory impairment.

In the absence of pathology, those with greater education have lower activation for performing the same task compared to those with lower education. In the presence of pathology, those with greater education can increase activation in response to pathology since they utilize fewer resources prior to pathology. In the presence of pathology, those with lower education cannot increase activation any further in response to pathology since they have heightened neural activation.

However, AD pathology is not independently accumulated, rather many patients that have increasing AD pathology (e.g., Aβ) also have cerebrovascular disease pathology, primarily white matter hyperintensities (WMHs). One study noted that AD rarely (~9%) occurred in isolation of other neuropathologies.[26] Thus, it is critical to investigate changes in WMH in late-life disorders to delineate AD and cerebrovascular disease pathology.

Using a cross-sectional study design in cognitively healthy older participants, we investigated the associations between fMRI activation during a working memory task (digit-symbol substitution task [DSST]), Aβ deposition, cognitive performance, WMH burden, and education.[27] These associations have not been established in cognitively healthy individuals. We chose DSST as it robustly activates the prefrontal cortex[28] and measures working memory which is associated with preclinical AD[29] and Aβ[30] in cognitively healthy individuals. We hypothesized that the greater neural activation during DSST would be associated with greater Aβ to compensate for accumulating pathology and maintain healthy cognitive function. Since our sample is cognitively healthy, DSST activation will not be associated with cognitive function since this activation largely serves to maintain healthy cognitive function. We hypothesize that those with greater education have more efficient activation - that is, lower activation for conducting the same task. We further hypothesized that this would not be dependent on WMH burden and is primarily associated with AD-like pathology.

METHODS

Participants

We recruited 50 community dwelling adults (>65 years) via advertisements or mailings to individuals interested in aging research. Participants completed a positron emission tomography (PET) Pittsburgh compound B (PiB) imaging scan, MRI, and neuropsychological assessment. Participants gave written informed consent prior to enrolling. The University of Pittsburgh Institutional Review Board approved this study.

Inclusion criteria were: greater than 65 years old, fluent in English, and if female they must be post-menopausal. Exclusion criteria were: presence of dementia or mild cognitive impairment (MCI, see Neuropsychological Assessment Battery), history of major neurologic or psychiatric disease, Geriatric Depression Scale greater than 15,[31] psychoactive medication use, contraindications to MRI, or have visual/auditory/motor deficits which may prevent the completion of behavioral testing.

Neuropsychological Assessment Battery

Participants underwent neuropsychological assessment examining memory, visuospatial construction, language, attention, and executive functions. Criteria for clinical impairment (MCI) were consistent with those implemented at the University of Pittsburgh Alzheimer Disease Research Center and included the following: performance on greater than or equal to 2 tests (within domain) or greater than or equal to 3 tests (across domains) below expectations (>1 SD, standard deviation, below age and education adjusted means); supported by participant reports of changes, memory or cognitive function concerns, or behavioral observations by staff. Blinded neuropsychologists (BES) and geriatric psychiatrists (WEK and HJA) reviewed results and clinical diagnosis was reached by consensus.

The Mini-Mental State Examination was administered as a global cognitive function measure.[32] The Consortium to Establish a Registry for Alzheimer Disease, word list learning recall was administered (immediate and delayed recall of words).[33] Visual memory was measured by the immediate and delayed recall of a modified Rey-Osterrieth complex figure.[34]

Attention and executive working memory were measured by the Trail Making Test (difference in seconds, Trails [B-A])[35] as well as the Wechsler Adult Intelligence Scale-Revised (WAIS-R) Digit Symbol ($DSST_{out}$; performed outside the scanner).[36] To measure inhibition we used the Stroop (Stroop) Color/ Word Interference test.[37]

The following tests were also administered to determine MCI/dementia, but were not used in the analysis: Clock drawing,[38] modified block design subtest from WAIS-R,[39] Boston Naming test,[40] Letter/ Category Fluency,[35] and digit spans forward or backward from WAIS-R.[36]

MRI Data Collection

We used a 3T Siemens Trio TIM scanner and 12 channel head coil. Sagittal whole brain 3D magnetization prepared rapid-acquisition gradient echo (MPRAGE) was collected with echo time (TE) = 2.98 msec, repetition time (TR) = 2,300 msec, flip angle (FA) = 9°, field of view (FOV) = 256 × 240, 1 × 1 × 1.2 mm resolution, 0.6 mm gap, and GeneRalized Autocalibrating Partial Parallel Acquisition (GRAPPA) acceleration factor = 2. Axial whole brain 2D fluid attenuated inversion recovery (FLAIR) was collected to measure WMH burden with TE = 90 msec, TR = 9,160 msec, FA = 150°, FOV = 212 × 256, 1 × 1 × 3 mm resolution, no gap, and GRAPPA = 2. Axial echo-planar imaging blood oxygen-level dependent (during DSST) was collected with TE = 32 msec, TR = 2,000 msec, FA = 90°, FOV = 128 × 128, 2 × 2 × 4 mm resolution, no gap, GRAPPA = 2, and 280 volumes. Due to low coverage and placement issues, we had no coverage of the cerebellum, top of the motor or supplemental motor cortex. A fieldmap was collected to correct for spatial distortion with TElow = 4.92 msec and TE-high = 7.38 msec (difference = phase image).

Digit Symbol Substitution Task (DSST) Within MRI Scanner

The computerized version of DSST,[27,31,41] used previously,[28] was completed in the MRI. Two keypads in each hand tracked responses. Participants see a number-symbol matching pair (cue) then see an answer key (probe) containing four number-symbol pairs. They push the right index finger if the probe contains one matched cue and push the left index finger if there are no matches and are asked to do so “as fast and accurately as you possibly can.” It is block design with 8 trials per block, alternated with control button pressing (participants either saw “RRRR” or “LLLL” for right or left, respectively) for a total of 10 blocks (5 experimental and 5 control). Each block lasts 56 seconds (total 9 minutes and 20 seconds). Cues were presented via E-prime,[42] and a mirror was used to present a computer screen to participants.

PET Scanning: PiB

PiB was synthesized by a simplified radiosynthetic method based on the captive solvent method.[43] Prior to acquisition, 15 mCi of high specific activity (~2.1 Ci/μmol at EOS) [^{11}C]PiB was injected intravenously over 20 seconds. A 10–15 minutes windowed transmission scan was acquired for attenuation correction, followed by a 20-minute emission scan (4 × 300 second frames) beginning 50 minutes postinjection. Data were acquired on a Siemens/CTI ECAT HR + scanner (Siemens Medical Solutions, Knoxville, TN) in 3D mode (63 axial imaging planes, FOV 15.2 cm, inplane resolution 4.1 mm full-width at half-maximum at FOV center, axial slice width 2.4 mm). Scanner is equipped with a neuro-insert to reduce scattered photon contribution. PET emission data were reconstructed using filtered back projection correcting for attenuation, scatter, and radionuclide decay.

PET Processing

Hand-drawn regions using MPRAGE were defined, which include frontal cortex (ventral and dorsal), anterior cingulate (subgenual and pregenual), anteroventral striatum, mesial temporal (hippocampus and amygdala), precuneus or posterior cingulate (ventral, middle, and dorsal), parietal cortex, lateral temporal, occipital (calcarine and pole), and cerebellum.

[44] PET-MR co-registration was performed using the automated image registration algorithm for alignment and reslicing.[45]

The dynamic [^{11}C]PiB acquisition frames are inspected for interframe motion. If suspected, the automated image registration algorithm (optimized for PET-to-PET registration) is applied on a framewise basis. A summed image over the postinjection interval is computed and a spatial transformation is applied, which is resliced in MPRAGE space. Volumes of interest (on MPRAGE) are used to extract regional concentrations, which are transformed into units of standardized uptake value (SUV) using the injected dose of [^{11}C]PIB and the participant's mass. The SUV outcome is normalized to nonspecific uptake (cerebellum), yielding an SUV ratio (SUVR) measure that compares favorably to fully quantitative measures.[46] Regional SUVR were partial volume corrected using a previously validated method that corrects for the dilution of PET signal due to limited spatial resolution.[47–50] A two-component approach corrects for the dilutional effect of expanded cerebrospinal fluid spaces accompanying normal aging and disease-related cerebral atrophy using FSL software (University of Oxford, Oxford, UK). A global PiB retention index reflecting cerebral amyloid load is computed from a weighted average of the SUVR values from the six most relevant regions. Participants were classified as PiB positive or negative using a threshold previously determined by using a sparse kmeans cluster analysis.[51]

MRI Processing

All data were preprocessed using Statistical Parametric Mapping software.[52] All image space interpolation was performed using fourth degree Bspline method and similarity metric for registrations was mutual information (for motion correction) or normalized mutual information (co-registration between different image types). A voxel displacement map was generated using the fieldmap, which was input into a motion correction algorithm (rigid; mean reference). The structural MRI was then co-registered to the mean functional image (affine). This image (after bias correction) was segmented, which outputs a deformation field that was used to normalize the functional images to Montreal Neurological Institute space (2 mm isotropic resolution). These data were smoothed using a Gaussian kernel (full-width at half-maximum 8 mm).

We used ART (https://www.nitrc.org/projects/artifact_detect/) to quantify the level of motion across participants. The median (interquartile range) of the following measures was minimal: max translational motion 1.31 (1.5), max range of translational motion 1.63 (1.7), average root mean square motion 1.41 (1.1), average scan-to-scan motion across the session 0.18 (0.1), and percent of TRs with head jerks (>0.5 mm for combined translations and rotations) was 7.0 (20.1). These were not significantly different between PiB positive and negative groups for max translational motion $t(48) = 0.03$, $p = 0.9712$, max range of translational motion $t(48) = 0.10$, $p = 0.9199$, average root mean square motion $t(48) = 0.87$, $p = 0.3896$, average scan-toscan motion $t(48) = 0.49$, $p = 0.6263$, and percent head jerks $t(48) = 0.71$, $p = 0.4818$.

The FLAIR was used to segment WMH. An automated skull stripping procedure was applied to the FLAIR using FSL's brain extraction tool (FMRIB software library[53]), which was manually corrected using ITK-SNAP.[54] A previously validated method was utilized for

WMH segmentation on the skull stripped FLAIR,[55] which identifies seeds above a specified standard deviation of intensities and then uses fuzzy connectedness to grow the seeds. The WMH volume is divided by the intracranial volume to get a normalized measure of WMH burden (the log of WMH is used in subsequent regressions).

Modeling DSST

We modeled the effect of the experimental and control conditions (convolved with the hemodynamic response function) using a general linear model. We included a high-pass filter (1/128 Hz to account for drift) as well as an autoregressive [AR(1)] model (to account for serial correlations due to aliased biorhythms or unmodeled activity). The contrast experimental minus control was computed and used in all subsequent group analyses.

Statistical Analysis

Our main variables of interest included education, global PiB, neurocognitive tests, and WMH burden. We adjusted for age, sex, and mean reaction time (RT) during in-scanner DSST. Descriptive statistics such as means (SD) were calculated in R[56] for all variables between PiB positive and negative groups. To test differences between groups, two-sample *t* tests or χ^2 (or Fisher's exact test) were used for continuous or categorical variables, respectively.

We performed a one-sample *t* test on experimental minus control contrast (for in-scanner DSST) to find regions that activated during the task. For all subsequent analyses, our tests were limited to regions that were activated by the task. Using simple linear regression models, we tested the associations between DSST activation and each of the following variables: education, global PiB, neurocognitive measures, and WMH burden. The variables that were significantly associated with the DSST activation in the univariate models were then included in a multiple regression model along with their interactions. In addition, we also explored if DSST activation in the scanner was associated with age, sex, or mean RT (in-scanner DSST) using simple linear regression.

To control for multiple comparisons, we used statistical nonparametric mapping toolbox.[57] We performed voxel-wise permutation testing (5,000 permutations) using a cluster forming p value <0.001[58] and used cluster-wise inference to control the family wise error rate at α less than 0.05.

Neuroimaging results were visualized either in BrainNet viewer[59] or xjview[60] with a single participant image. To better interpret each of the significant clusters, we separated each cluster structurally using the automatic anatomic labeling template and labeled each as a Brodmann area if greater than 20% of that cluster overlapped with a Brodmann area. We also included whether clusters belonged to common neural networks using a previously established set of functional resting state networks (defined using independent components analysis)[61] that were threshold at a Z-value greater than or equal to 3 and a minimum cluster size of 50 voxels. We then determined whether each cluster was part of (>20% cluster overlap) any of five networks of interest (anterior salience, dorsal or ventral default mode or left/right executive control). This was done only to better understand the spatial extent of identified clusters with respect to common neural networks.

RESULTS

Table 1 shows the demographic and cognitive measures by PiB status. The PiB positive group performed worse on the Trails(B-A) and had a greater percentage of Caucasian participants (85% compared to 81%), but there were no other group differences including WMH.

All significant group voxel-wise analyses are shown in Table 2. The task significantly activated (see Table 2 and Fig. 1) the visual cortex, motor and sensory, parietal cortex, angular/precuneus/supramarginal, inferior or middle temporal, cerebellum, thalamus, caudate, hippocampus, putamen, insula, fusiform gyrus, anterior or middle cingulate, as well frontal cortex (inferior, middle, and superior frontal clusters). We found that DSST activation in the scanner was not associated with age, sex, or mean RT (in-scanner DSST).

We found a significant positive association between continuous (but not dichotomous) global PiB SUVR and DSST activation in multiple regions. Further, we found that education was negatively associated with the left inferior temporal gyrus ($x = 36$, $y = 40$, $z = 2$, $t_{max} = 4.7$, 250 voxels). We found no associations between DSST activation and the out-of-scanner cognitive tests or WMH burden.

Our multiple regression model included PiB, education as well as their interaction. The interaction was not significant thus, our final model included PiB and education. In this final model, education was no longer significant; but PiB remained significant (see Table 2 and Fig. 2). DSST activation in the right calcarine, precuneus, middle temporal, left insula, and inferior frontal gyrus (operculum) was positively associated with greater global PiB retention (plotted in Fig. 3).

To understand the relative effect sizes of these associations, we visualized the voxel-wise Pearson's correlation between each variable of interest and DSST activation in Fig. 4. This was not an additional analysis, rather a visual representation of the voxel-wise effect sizes for each of the univariate models described in the statistical analysis section. The violin plots are histograms (mirrored on the vertical axis) of the univariate correlations across all voxels to show how many voxels have a relatively small (0.3) or medium (0.5) effect size.

DISCUSSION

DSST robustly activated a network of regions involved in cognitive control, attention, and working memory.[62] We found that greater Ab burden was associated with greater DSST activation in the insula, inferior frontal gyrus, precuneus, calcarine, and middle temporal gyrus in cognitively healthy individuals. Greater education was associated with lower activation; however, this effect was not significant when adjusting for Ab burden. DSST activation was not associated with cognitive function or WMH burden. This may suggest that greater DSST activation may compensate for greater Ab burden to maintain healthy cognitive function. We extend on past literature that have shown these associations in clinical populations to cognitively healthy individuals during the preclinical stage. Lower activation was associated with greater education which may represent more efficient neural network processing even if at this stage Aβ burden is the primary correlate of activation.

We found that greater DSST activation was associated with greater Aβ burden, which has previously been reported.[63] This effect seems to be localized to nodes of the DMN, which reflects the early spatial pattern of Aβ accumulation.[16,20] The association between Aβ burden with insula activation may reflect its role in working memory.[64] Previous work has demonstrated that insula activation is associated with episodic memory decline.[12,65,66]

Previous studies have reported increased fMRI activation in the hippocampus in preclinical AD[67] and MCI.[68] One explanation posed for this finding is pathology-induced compensation, in which cognitive decline is prevented or delayed by increased activation (a "state" model). In this model, individuals with greater cognitive reserve (e.g., greater education) show increased activation in the presence of pathology to compensate and maintain healthy cognitive function. A competing explanation holds that those with greater cognitive reserve (e.g., greater education) have greater activation prior to any pathology (a "trait" model).[69] We demonstrate that in cognitively healthy individuals, those with greater education have lower activation and that greater Aβ burden is associated with greater activation, which is in-line with the state model.

Figure 4 demonstrates the relatively higher correlation between DSST activation and amyloid burden and education, but relatively weak associations with current cognitive performance. In this preclinical stage, the association between activation and cognitive performance is weak possibly because neural network activation is capable of compensation to prevent or delay cognitive decline. This also demonstrates the weaker associations with other variables outside of PiB in this preclinical stage and may explain the effect of PiB on the association between education and DSST activation.

Consistent with our previous reports,[70,71] we found no cross-sectional association between Aβ deposition and cognitive function as well as WMH burden, except for an association with the Trail Making Test. This, however, was not associated with activation and so the relationship between Aβ, activation during working memory tasks, and set shifting is unclear. Previous studies have also reported absence of an association between Aβ and cognitive function especially when utilizing cross-sectional study designs in cognitively healthy older individuals.[21]

Limitations of this study include a relatively small sample size with relatively few individuals that were amyloid positive (N = 13). While we found no group differences (Aβ positive versus negative), we did find that DSST activation was associated with Aβ continuously, further reflecting either the small sample size or the uneven groups. We investigated associations between neural activation and Aβ as well as education, as such we cannot make any causal inferences of the nature of these associations. Due to the design of the fMRI task, deactivations (or relative decreases in fMRI signal) during DSST could not be evaluated. Education was not significant after adjusting for PiB, suggesting a weak association in cognitive healthy individuals, thus the interpretation of cognitive reserve needs to be further validated. Education itself is only one proxy of cognitive reserve and is not sufficient to explain its impact. Other measures like premorbid IQ and occupational attainment have also been used as proxy and explain unique variance in predicting AD risk.[25] Thus, future studies should use more sophisticated proxies of reserve that may combine

measures of education, IQ, literacy level, number of intellectually stimulating leisure activities, degree of occupational complexity and attainment, and socioeconomic status. Further, we interpret the loss of the statistical significance of education after the addition of the major neuropathologic variable (Aβ) as compensation, since this indicates that while education may be playing a role in this early period, factors like Aβ may be the major correlates of neural activation. This compensation hypothesis however should be properly tested with a sample that has varying levels of pathology and cognitive function (i.e., including those with cognitive impairment). Ideally, a longitudinal study may be able to fully clarify whether this association holds in a preclinical sample that converts to AD.

This study supports previously identified relationships between Aβ and functional brain activation in cognitively healthy older participants, which we expand to include associations between working memory neural activation and Aβ. We show that increased Ab is associated with increased activation in the insula, inferior frontal gyrus, precuneus, and middle temporal cortex. This may be a compensatory mechanism to maintain normal cognitive function even in the presence of high Aβ burden.

Acknowledgments

This study was supported by funding from NIA P50 AG005133, R37 AG025516, P01 AG025204, 5K23AG038479, R01 MH076079, and NIMH T32 MH019986. GE Healthcare holds a license agreement with the University of Pittsburgh based on the technology described in this manuscript. Drs. Klunk and Mathis are co-inventors of PiB and, as such, have a financial interest in this license agreement. GE Healthcare provided no grant support for this study and had no role in the design or interpretation of results or preparation of the manuscript. The other authors declare no conflicts of interest.

References

1. Hardy J, Selkoe DJ: The amyloid hypothesis of Alzheimer’s disease: progress and problems on the road to therapeutics. Science 2002; 297:353–356 [PubMed: 12130773]
2. Selkoe DJ: The molecular pathology of Alzheimer’s disease. Neuron 1991; 6:487–498 [PubMed: 1673054]
3. Roberson ED, Scearce-Levie K, Palop JJ, et al.: Reducing endogenous tau ameliorates amyloid beta-induced deficits in an Alzheimer’s disease mouse model. Science 2007; 316:750–754 [PubMed: 17478722]
4. Stancu IC, Vasconcelos B, Terwel D, et al.: Models of beta-amyloid induced Tau-pathology: the long and “folded” road to understand the mechanism. Mol Neurodegener 2014; 9:51 [PubMed: 25407337]
5. Bateman RJ, Xiong C, Benzinger TL, et al.: Clinical and biomarker changes in dominantly inherited Alzheimer’s disease. N Engl J Med 2012; 367:795–804 [PubMed: 22784036]
6. Fleisher AS, Chen K, Quiroz YT, et al.: Florbetapir PET analysis of amyloid-beta deposition in the presenilin 1 E280A autosomal dominant Alzheimer’s disease kindred: a cross-sectional study. Lancet Neurol 2012; 11:1057–1065 [PubMed: 23137949]
7. Jack CR Jr., Knopman DS, Jagust WJ, et al.: Tracking pathophysiological processes in Alzheimer’s disease: an updated hypothetical model of dynamic biomarkers. Lancet Neurol 2013; 12:207–216 [PubMed: 23332364]
8. Hedden T, Oh H, Younger AP, et al.: Meta-analysis of amyloid-cognition relations in cognitively normal older adults. Neurology 2013; 80:1341–1348 [PubMed: 23547267]
9. Fagan AM, Roe CM, Xiong C, et al.: Cerebrospinal fluid tau/beta-amyloid(42) ratio as a prediction of cognitive decline in nondemented older adults. Arch Neurol 2007; 64:343–349 [PubMed: 17210801]

10. Landau SM, Mintun MA, Joshi AD, et al.: Amyloid deposition, hypometabolism, and longitudinal cognitive decline. Ann Neurol 2012; 72:578–586 [PubMed: 23109153]
11. Lim YY, Maruff P, Pietrzak RH, et al.: Effect of amyloid on memory and non-memory decline from preclinical to clinical Alzheimer's disease. Brain 2014; 137:221–231 [PubMed: 24176981]
12. Resnick SM, Sojkova J, Zhou Y, et al.: Longitudinal cognitive decline is associated with fibrillar amyloid-beta measured by [11C]PiB. Neurology 2010; 74:807–815 [PubMed: 20147655]
13. Mormino EC, Betensky RA, Hedden T, et al.: Synergistic effect of beta-amyloid and neurodegeneration on cognitive decline in clinically normal individuals. JAMA Neurol 2014; 71:1379–1385 [PubMed: 25222039]
14. Knopman DS, Jack CR Jr., Wiste HJ, et al.: Selective worsening of brain injury biomarker abnormalities in cognitively normal elderly persons with beta-amyloidosis. JAMA Neurol 2013; 70: 1030–1038 [PubMed: 23797806]
15. Hedden T, Van Dijk KR, Becker JA, et al.: Disruption of functional connectivity in clinically normal older adults harboring amyloid burden. J Neurosci 2009; 29:12686–12694 [PubMed: 19812343]
16. Sheline YI, Raichle ME, Snyder AZ, et al.: Amyloid plaques disrupt resting state default mode network connectivity in cognitively normal elderly. Biol Psychiatry 2010; 67:584–587 [PubMed: 19833321]
17. Mormino EC, Smiljic A, Hayenga AO, et al.: Relationships between beta-amyloid and functional connectivity in different components of the default mode network in aging. Cereb Cortex 2011; 21:2399–2407 [PubMed: 21383234]
18. Elman JA, Oh H, Madison CM, et al.: Neural compensation in older people with brain amyloid-beta deposition. Nat Neurosci 2014; 17:1316–1318 [PubMed: 25217827]
19. Nelissen N, Vandenbulcke M, Fannes K, et al.: Abeta amyloid deposition in the language system and how the brain responds. Brain 2007; 130:2055–2069 [PubMed: 17586869]
20. Lim HK, Nebes R, Snitz B, et al.: Regional amyloid burden and intrinsic connectivity networks in cognitively normal elderly subjects. Brain 2014; 137:3327–3338 [PubMed: 25266592]
21. Jagust W: Is amyloid-beta harmful to the brain? Insights from human imaging studies. Brain 2016; 139:23–30 [PubMed: 26614753]
22. Rieck JR, Rodrigue KM, Kennedy KM, et al.: The effect of beta-amyloid on face processing in young and old adults: a multivariate analysis of the BOLD signal. Hum Brain Mapp 2015; 36: 2514–2526 [PubMed: 25832770]
23. Rentz DM, Amariglio RE, Becker JA, et al.: Face-name associative memory performance is related to amyloid burden in normal elderly. Neuropsychologia 2011; 49:2776–2783 [PubMed: 21689670]
24. Stern Y: Cognitive reserve in ageing and Alzheimer's disease. Lancet Neurol 2012; 11:1006–1012 [PubMed: 23079557]
25. Barulli D, Stern Y: Efficiency, capacity, compensation, maintenance, plasticity: emerging concepts in cognitive reserve. Trends Cogn Sci 2013; 17:502–509 [PubMed: 24018144]
26. Boyle PA, Yu L, Wilson RS, et al.: Person-specific contribution of neuropathologies to cognitive loss in old age. Ann Neurol 2018; 83:74–83 [PubMed: 29244218]
27. Salthouse TA: The role of memory in the age decline in digit-symbol substitution performance. J Gerontol 1978; 33:232–238 [PubMed: 637915]
28. Venkatraman VK, Aizenstein H, Guralnik J, et al.: Executive control function, brain activation and white matter hyperintensities in older adults. Neuroimage 2010; 49:3436–3442 [PubMed: 19922803]
29. Backman L, Jones S, Berger AK, et al.: Cognitive impairment in preclinical Alzheimer's disease: a meta-analysis. Neuropsychology 2005; 19:520–531 [PubMed: 16060827]
30. Baker JE, Lim YY, Pietrzak RH, et al.: Cognitive impairment and decline in cognitively normal older adults with high amyloid-beta: a meta-analysis. Alzheimers Dement (Amst) 2017; 6:108–121 [PubMed: 28239636]
31. Yesavage JA, Brink TL, Rose TL, et al.: Development and validation of a geriatric depression screening scale: a preliminary report. J Psychiatr Res 1982; 17:37–49 [PubMed: 7183759]

32. Folstein MF, Folstein SE, McHugh PR, et al.: Mini-Mental State Examination: MMSE user's guide. Psychology Assessment Resources, 2000
33. Morris J, Edland S, Clark C, et al.: The consortium to establish a registry for Alzheimer's disease (CERAD). Neurology 1993; 43: 2457–2465 [PubMed: 8255439]
34. Becker JT, Boller F, Saxton J, et al.: Normal rates of forgetting of verbal and non-verbal material in Alzheimer's disease. Cortex 1987; 23:59–72 [PubMed: 3568706]
35. Strauss E, Sherman EM, Spreen O: A Compendium of Neuropsychological Tests: Administration, Norms, and Commentary. American Chemical Society, 2006
36. Wechsler D: WAIS-R Manual: Wechsler Adult Intelligence Scale-Revised. Psychological Corporation, 1981
37. Golden CJ: A manual for the clinical and experimental use of the Stroop color and word test. 1978;
38. Freedman M: Clock Drawing: A Neuropsychological Analysis. USA: Oxford University Press, 1994
39. Lopez OL, Becker JT, Jagust WJ, et al.: Neuropsychological characteristics of mild cognitive impairment subgroups. J Neurol Neurosurg Psychiatry 2006; 77:159–165 [PubMed: 16103044]
40. Kaplan E, Goodglass H, Weintraub S: Boston Naming Test. Proed, 2001
41. Matarazzo JD, Herman DO: Base rate data for the WAIS-R: testretest stability and VIQ-PIQ differences. J Clin Neuropsychol 1984; 6:351–366 [PubMed: 6501578]
42. Schneider W, Eschman A, Zuccolotto A: E-Prime: User's guide. Psychology Software Incorporated, 2002
43. Wilson AA, Garcia A, Jin L, et al.: Radiotracer synthesis from [(11) C]-iodomethane: a remarkably simple captive solvent method. Nucl Med Biol 2000; 27:529–532 [PubMed: 11056365]
44. Cohen AD, Price JC, Weissfeld LA, et al.: Basal cerebral metabolism may modulate the cognitive effects of Abeta in mild cognitive impairment: an example of brain reserve. J Neurosci 2009; 29:14770–14778 [PubMed: 19940172]
45. Woods RP, Mazziotta JC, Cherry SR: MRI-PET registration with automated algorithm. J Comput Assist Tomogr 1993; 17:536–546 [PubMed: 8331222]
46. Lopresti BJ, Klunk WE, Mathis CA, et al.: Simplified quantification of Pittsburgh Compound B amyloid imaging PET studies: a comparative analysis. J Nucl Med 2005; 46:1959–1972 [PubMed: 16330558]
47. Meltzer CC, Zubieta JK, Links JM, et al.: MR-based correction of brain PET measurements for heterogeneous gray matter radioactivity distribution. J Cereb Blood Flow Metab 1996; 16:650–658 [PubMed: 8964805]
48. Meltzer CC, Smith G, Price JC, et al.: Reduced binding of [18F]altanserin to serotonin type 2A receptors in aging: persistence of effect after partial volume correction. Brain Res 1998; 813:167–171 [PubMed: 9824691]
49. Meltzer CC, Cantwell MN, Greer PJ, et al.: Does cerebral blood flow decline in healthy aging? A PET study with partial-volume correction. J Nucl Med 2000; 41:1842–1848 [PubMed: 11079492]
50. Price JC, Klunk WE, Lopresti BJ, et al.: Kinetic modeling of amyloid binding in humans using PET imaging and Pittsburgh Compound-B. J Cereb Blood Flow Metab 2005; 25:1528–1547 [PubMed: 15944649]
51. Cohen AD, Mowrey W, Weissfeld LA, et al.: Classification of amyloid-positivity in controls: comparison of visual read and quantitative approaches. Neuroimage 2013; 71:207–215 [PubMed: 23353602]
52. Ashburner J, Barnes G, Chen C-c, et al.: SPM12 Manual The FIL Methods Group (and honorary members). 2014;
53. Smith SM: Fast robust automated brain extraction. Hum Brain Mapp 2002; 17:143–155 [PubMed: 12391568]
54. Yushkevich P: ITK-SNaP Integration. NLM Insight, 2006 Webpage http://www.itk.org/index.htm. Accessed July 27, 2005
55. Wu M, Rosano C, Butters M, et al.: A fully automated method for quantifying and localizing white matter hyperintensities on MR images. Psychiatry Res 2006; 148:133–142 [PubMed: 17097277]

56. Team RC: R: A Language and Environment for Statistical Computing. Vienna, Austria: R Foundation for Statistical Computing, 2013:2014
57. Nichols TE, Holmes AP: Nonparametric permutation tests for functional neuroimaging: a primer with examples. Hum Brain Mapp 2002; 15:1–25 [PubMed: 11747097]
58. Eklund A, Nichols TE, Knutsson H: Cluster failure: why fMRI inferences for spatial extent have inflated false-positive rates. Proc Natl Acad Sci U S A 2016; 113:7900–7905 [PubMed: 27357684]
59. Xia M, Wang J, He Y: BrainNet Viewer: a network visualization tool for human brain connectomics. PLoS One 2013; 8:e68910 [PubMed: 23861951]
60. Cui X, Li J, Song X: xjview: a viewing program for SPM. Retreived from www.alivelearn.net/xjview8, 2011
61. Smith SM, Fox PT, Miller KL, et al.: Correspondence of the brain's functional architecture during activation and rest. Proc Natl Acad Sci U S A 2009; 106:13040–13045 [PubMed: 19620724]
62. Samartsidis P, Eickhoff CR, Eickhoff SB, et al.: Bayesian logGaussian Cox process regression: applications to meta-analysis of neuroimaging working memory studies. J R Stat Soc 2018; 68:217–234
63. Mormino EC, Brandel MG, Madison CM, et al.: Abeta Deposition in aging is associated with increases in brain activation during successful memory encoding. Cereb Cortex 2012; 22:1813–1823 [PubMed: 21945849]
64. Owen AM, McMillan KM, Laird AR, et al.: N-back working memory paradigm: a meta-analysis of normative functional neuroimaging studies. Hum Brain Mapp 2005; 25:46–59 [PubMed: 15846822]
65. Xie C, Bai F, Yu H, et al.: Abnormal insula functional network is associated with episodic memory decline in amnestic mild cognitive impairment. Neuroimage 2012; 63:320–327 [PubMed: 22776459]
66. Schwindt GC, Black SE: Functional imaging studies of episodic memory in Alzheimer's disease: a quantitative meta-analysis. Neuroimage 2009; 45:181–190 [PubMed: 19103293]
67. Sperling RA, Laviolette PS, O'Keefe K, et al.: Amyloid deposition is associated with impaired default network function in older persons without dementia. Neuron 2009; 63:178–188 [PubMed: 19640477]
68. Huijbers W, Mormino EC, Schultz AP, et al.: Amyloid-beta deposition in mild cognitive impairment is associated with increased hippocampal activity, atrophy and clinical progression. Brain 2015; 138:1023–1035 [PubMed: 25678559]
69. Aizenstein HJ, Klunk WE: Where is hippocampal activity in the cascade of Alzheimer's disease biomarkers? Brain 2015; 138: 831–833 [PubMed: 25802317]
70. Klunk WE, Price JC, Mathis CA, et al.: Amyloid deposition begins in the striatum of presenilin-1 mutation carriers from two unrelated pedigrees. J Neurosci 2007; 27:6174–6184 [PubMed: 17553989]
71. Nebes RD, Snitz BE, Cohen AD, et al.: Cognitive aging in persons with minimal amyloid-beta and white matter hyperintensities. Neuropsychologia 2013; 51:2202–2209 [PubMed: 23911776]

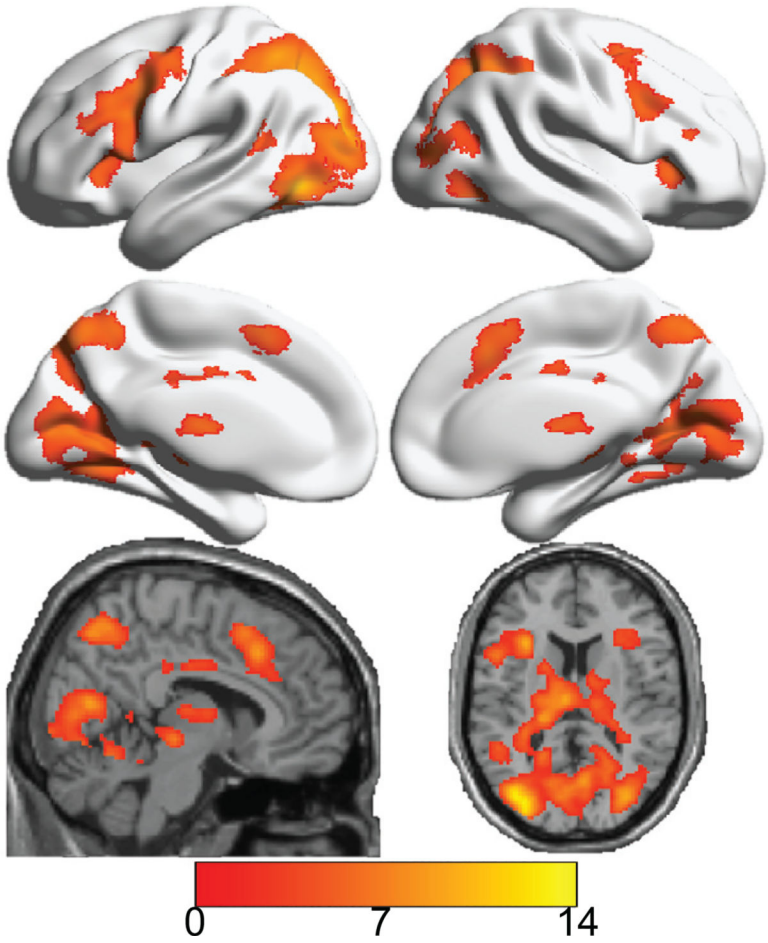

FIGURE 1.

Main effect of the in-scanner DSST using a one-sample *t* test across the entire sample (testing for regions that are significantly activated in the experimental compared to the control condition). Color bar indicates value of t-statistic (for one-sample *t* test), where red/orange values indicate areas that were significantly activated by task (relative to control) and blue values indicate areas that were significantly activated by control (relative to task − none). Cortical regions are shown on the surface of a brain while subcortical regions are shown on a single participant structural (from the standard space anatomic images in SPM). As expected, the in-scanner DSST activated multiple regions reliably including visual processing areas (primary and secondary), subcortical regions (thalamus/caudate), motor and supplemental motor, as well as a large number of central executive areas (including dorsolateral prefrontal cortex, dlPFC).

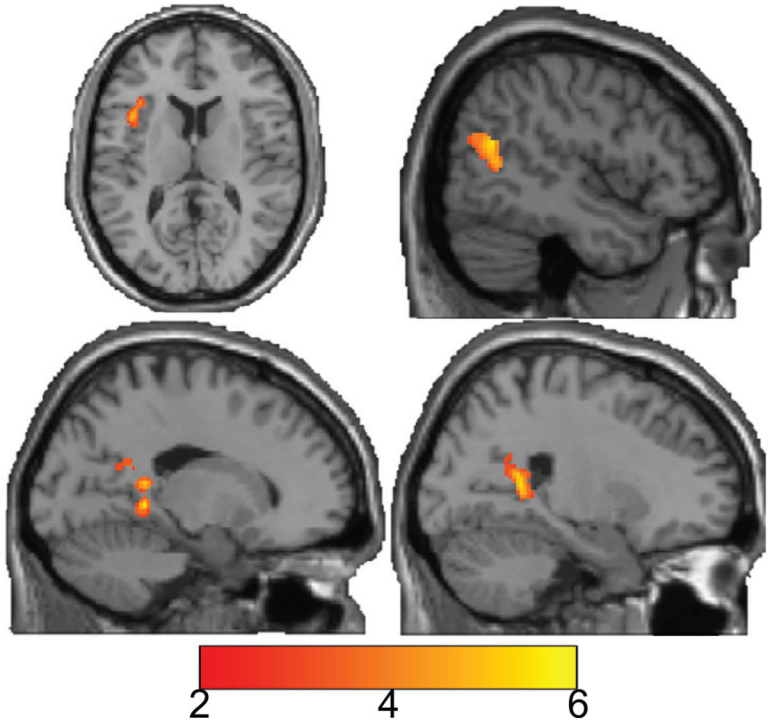

FIGURE 2.

Association between in-scanner DSST activation (novel-control) and PiB while adjusting for education. Results are shown on a single participant structural (from the standard space anatomic images in SPM). Color bar indicates value of t-statistic (for regression), where red/orange values indicate areas of activation that were significantly positively associated ith PiB and blue values indicate areas where activation was significantly negatively associated with PiB (none). Greater PiB was associated with greater DSST activation (positive associations) in calcarine, middle temporal, precuneus, insula, and inferior frontal gyrus (operculum).

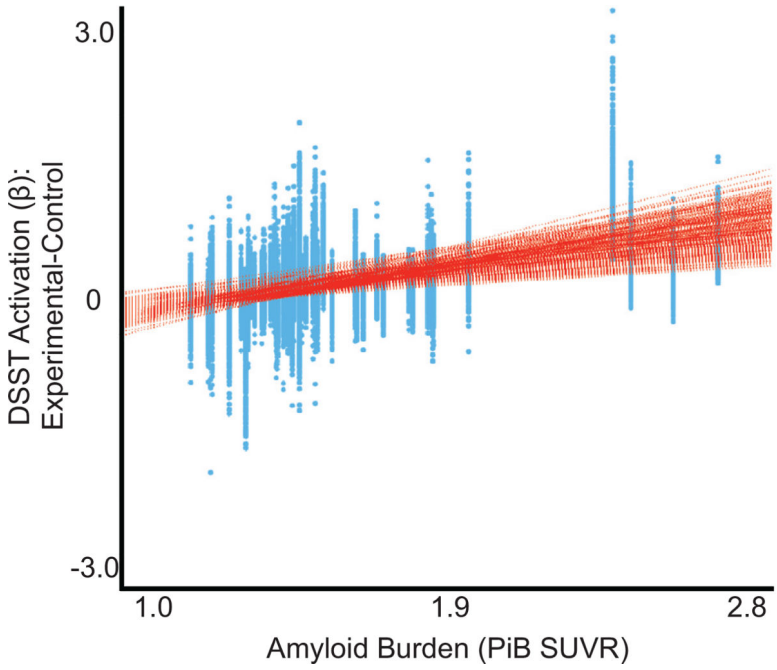

FIGURE 3.

Association between PiB SUVR and every voxel's DSST activation (experimental minus control contrast). This was done to show the range of the associations across all voxels. Greater Ab burden (PiB SUVR) was positively associated with increased DSST activation during the experimental condition (compared to the control).

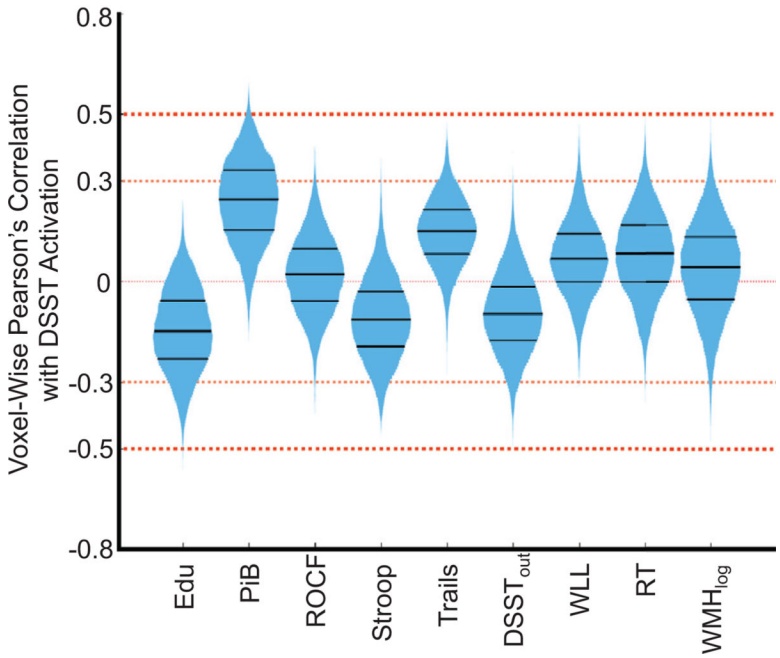

FIGURE 4.

Voxel-wise (only in area of main effect of the task) Pearson's correlation between DSST activation and each variable of interest. The violin plot reflects the histogram (mirrored on the vertical axis) of all voxel-wise correlations to show the relative effect sizes for each variable. The black bars inside the histogram reflect the 25th, 50th, and 75th percentiles. Notice that the PiB has the largest effect sizes with more than 25% of the voxels exceeding an effect size of 0.3 and a set exceeding 0.5. Thus, education has a small negative association while PiB has a medium positive association with neural activation. We can also see the relative associations between neural activation and each of the investigated variables.

TABLE 1.

Demographics and Summary Scores of Cognitive Measurements for this sample. We did not conduct a statistical test on Global PiB (SUVR) since this is how these groups were defined.

	PiB Positive (N = 13)	PiB Negative (N = 37)			
	Mean (SD)				
Variable	N (%)		**95% CI for Mean Difference**	**Test Statistic (df)**	**p Value**
Age (years)	77 (6)	75 (7)	(−7.4, 1.3)	$t(20.6) = -1.44$	0.16
Sex	6 M (46%)	13 M (35%)	NA	X(1) = 0.09	0.76
Race	**11 CC (85%)**	**30 CC (81 %)**	**NA**	**X(3) = 7.70**	**0.05**
Education (years)	14 (3)	15 (3)	(−0.7, 2.6)	$t(21) = 1.21$	0.24
MMSE	29 (2)	29 (1)	(−1.2, 1.3)	$t(16.3) = -0.07$	0.94
Boston Naming test (# spontaneously correct)	56.3 (5.3)	56.9 (3.9)	(−2.8, 4.2)	$t(15) = 0.41$	0.69
Letter fluency (# words, sum F, A, S)	48.3 (13.8)	42.5 (13.8)	(−16.1, 4.4)	$t(17.7) = -1.19$	0.25
Category fluency (# words in 60sec)	20.2 (5.3)	19.8 (4.6)	(−3.6, 2.7)	$t(24) = -0.29$	0.77
Global PiB (SUVR)	**2.03 (0.33)**	**1.44 (0.12)**	**(−0.8, −0.39)**		
ROCF (points, max 24)	16.6 (2.9)	15.7 (3.4)	(−1.13, 2.91)	$t(24.8) = 0.91$	0.37
Stroop (# correct)	10.9 (2.5)	12.5 (2.1)	(−0.1, 3.2)	$t(18) = 2.0$	0.06
Trails(B-A) (sec)	**104.8 (55.4)**	**70.7 (23.8)**	**(−68.6, −0.41)**	**$t(13.7) = -2.18$**	**0.05**
DSST (out) (# correct pairs)	46.1 (15.5)	52.8 (9.9)	(−2.98, 16.49)	$t(15.6) = 1.47$	0.16
WLL (words recalled)	7.4 (1.9)	7.3 (1.9)	(−1.46, 1.29)	$t(18.8) = -0.13$	0.90
DSST RT (Correct Trials-RT)	1509.7 (386.6)	1472.6 (246.4)	(−280.7, 206.4)	$t(15.6) = -0.32$	0.75
DSST percent accuracy	0.84 (0.15)	0.87 (0.12)	(−0.06, 0.13)	$t(17.3) = 0.70$	0.5

TABLE 2.

Significant Neuroimaging Results Showing the Analysis (Either Main Effect of the DSST Activation or Its Association With PiB Adjusting for Education), the Region Name, the Hemisphere, Brodmann Areas (With At Least 20% Cluster Overlap), Associated Network (With At Least 20% Cluster Overlap), Total Cluster Size (Number of Voxels), Maximum t-Statistic, and Location (x, y, z) in MNI Space

ROI	Region	Side	BA	Networks	Cluster Size	Max t	X, Y, Z (MNI)
Main effect of DSST activation	Angular	L	7, 39, 40	LECN, RECN, vDMN	148	7.3	−30, −50, 38
		R	7	LECN, vDMN	275	6.7	34, −56, 50
	Calcarine	L	17, 18		1094	6.2	−12, −72, 8
		R	17, 18	dDMN, vDMN	1100	6.4	16, −62, 6
	Caudate	L			214	6.7	−20, −16, 24
		R			238	5.7	20, 8, 20
	Cerebellum culmen	L	18, 19, 37		251	5.2	−20, −52, −16
		R	18, 30	vDMN	128	4.7	22, −44, −16
	Cerebellum culmen/declive	L	18, 19		167	5.8	−20, −56, −14
	Anterior cingulate	R	24, 32		59	4.1	10, 30, 28
	Middle cingulate	L	23, 32	ASN	189	4.4	2, 22, 38
		R	23, 32	LECN	423	5.8	6, 22, 42
	Cuneus	L	18, 19	dDMN	366	5.4	−18, −72, 36
		R	18	dDMN, vDMN	233	5.2	24, −62, 30
	Inferior frontal (operculum)	L	44, 48	RECN, vDMN	758	6.7	−38, 4, 28
		R	44, 48	LECN	422	6.0	38, 8, 32
	Inferior frontal (orbital)	L	47	RECN	52	5.0	−34, 26, −4
	Inferior frontal (triangular)	L	45, 48	RECN, vDMN	751	6.2	−46, 16, 32
		R	45, 48	LECN	335	4.9	36, 30, 4
	Middle frontal	L	6, 44	ASN, RECN, vDMN	248	7.9	−26, −2, 50
		R	6	LECN	426	6.3	30, 2, 56
	Superior frontal	L	6	ASN	95	7.4	−24, −2, 48
		R	6, 8	ASN, LECN, vDMN	87	6.0	28, 2, 56
	Superior medial frontal	L	32	LECN, RECN	70	5.3	2, 22, 44
	Fusiform	L	19, 37		677	9.3	−38, −62, −10
		R	19, 37	vDMN	429	7.0	32, −80, −2

ROI	Region	Side	BA	Networks	Cluster Size	Max t	X, Y, Z (MNI)
	Hippocampus	L	27, 37		203	5.1	−28, −32, 0
		R	27, 37		108	5.2	22, −32, 4
	Insula	L	47, 48		463	6.4	−30, 20, 12
		R	47, 48		330	5.4	32, 24, 0
	Lingual gyrus	L	18, 19		1126	6.3	−12, −70, 6
		R	17, 18, 19	vDMN	815	6.4	16, −60, 6
	Inferior occipital	L	19, 37		500	9.7	−40, −64, −8
		R	19		284	7.6	34, −80, −2
	Middle occipital	L	19	vDMN	2133	11.1	−30, −80, 28
		R	19	LECN, vDMN	1156	10.0	30, −76, 22
	Superior occipital	L	18, 19	dDMN, vDMN	511	8.5	−24, −72, 34
		R	7, 19	LECN, vDMN	587	9.8	30, −78, 22
	Inferior parietal	L	7, 40	ASN, RECN, vDMN	1399	9.0	−28, −60, 44
		R	40	ASN, LECN	423	6.3	34, −54, 50
	Superior parietal	L	7	ASN, RECN, vDMN	922	9.0	−26, −60, 44
		R	7	ASN, LECN, vDMN	332	6.6	24, −62, 50
	Postcentral	L	4, 6		252	5.9	−42, −8, 48
	Precentral	L	6	RECN, vDMN	1291	7.6	−28, −2, 50
		R	6	ASN, LECN	407	5.9	38, 6, 32
	Precuneus	L	7	ASN, dDMN, vDMN	1057	6.3	−4, −56, 54
		R	7	ASN, dDMN, LECN, vDMN	868	6.0	4, −62, 56
	Putamen	L	48		106	6.2	−22, 2, 16
	Supplemental Motor	L	6, 8, 32	RECN	358	5.7	−4, 10, 54
		R	6, 32	LECN	201	5.4	6, 14, 50
	Supramarginal	L	2, 48	ASN, RECN	85	5.7	−46, −34, 36
		R	40	ASN, LECN	53	5.4	44, −42, 44
	Inferior temporal	L	37		389	9.7	−46, −64, −6
		R	37	LECN	236	6.1	46, −60, −12
	Middle temporal	L	21, 37	ASN	637	8.5	−42, −58, −4
		R	37, 39	ASN, dDMN	198	4.9	40, −68, 22
	Thalamus	L			776	6.6	−4, −14, 10

ROI	Region	Side	BA	Networks	Cluster Size	Max t	X, Y, Z (MNI)
DSST activation association with PiB adjusting for education		R			537	5.5	20, −30, 6
	Cerebellum vermis	B	18		231	5.4	0, −48, −18
	Calcarine	R	28		78	4.7	22, −50, 14
	Inferior frontal (Operculum)	L	48		55	4.1	−40, 14, 14
	Insula	L	48	ASN	137	4.2	−32, 22, 16
	Precuneus	R	23	dDMN	115	4.8	6, −58, 24
	Middle temporal	R	47, 52	ASN, dDMN	267	4.6	46, −62, 18

ASN: anterior salience; dDMN/vDMN: dorsal or ventral default mode; LECN: left executive control; RECN: right executive control.